

# ALL CERAMIC CANTILEVER SENSORS WITH BORON CARBIDE LAYER: ADVANTAGES AND DIMENSIONAL LIMITATIONS

MYKOLA LUGOVY\*

*Institute for Problems of Materials Science, Kyiv, Ukraine*

*E-mail: [nil2903@gmail.com](mailto:nil2903@gmail.com)*

**Abstract** A model that predicts minimal length and thickness of all ceramic two layer cantilever sensors for chemical and biological detection is proposed. The model allows the estimation of minimal length and thickness where the conditions for the safe cantilever operation are satisfied. Two materials have been chosen for the consideration of the piezoelectric and non-piezoelectric layers in the layered cantilever. A piezoelectric material is lead zirconate titanate and a non-piezoelectric material is boron carbide. Different conditions, such as von Mises criterion and Mohr's strength theory are considered to find a safe stress level in the clamped cross-section of the cantilever.

**Keywords:** cantilever; ceramic; sensor; sensitivity; piezoelectric

## 1. Introduction

Biological and chemical sensors have a wide-range of applications in medical diagnoses, environmental surveillance, and pathogen and biological/chemical agent detection [1–4]. One type of the sensors available for temperature, surface stress, and mass detection is a piezoelectric microcantilever sensor, which transduces the recognition event from its surface into electrical signals further analyzed for the detection.

The piezoelectric microcantilever sensor consists of a piezoelectric layer bonded to a non-piezoelectric layer [5]. The adsorption of a target agent onto the piezoelectric material causes a change in the cantilever's mass, which in turn causes a shift in the resonance frequency [6, 7]. The sensitivity of piezoelectric microcantilever sensors is determined by the resonance frequency shift  $\Delta f$  per mass change  $\Delta m$  which depends on the effective

---

\* Mykola Lugovy, Institute for Problems of Materials Science, Kyiv, Ukraine, e-mail: [nil2903@gmail.com](mailto:nil2903@gmail.com)

elastic modulus, effective density of the cantilever and cantilever dimensions (length  $l$ , width  $w$ ).  $\Delta f / \Delta m$  will increase with decreasing cantilever dimensions and density, and with increasing elastic modulus [5].

Lead zirconate titanate (PZT) is a material's choice for the piezoelectric layer of microcantilever ( $E = 61$  GPa,  $\rho = 7.5$  g/cm<sup>3</sup> [5]). For the non-piezoelectric layer, a stainless steel ( $E = 200 - 250$  GPa,  $\rho = 7.7 - 8$  g/cm<sup>3</sup>) is frequently used [4]. However, if the non-piezoelectric ceramic layer in the microcantilever layered structure could be replaced with a material of higher elastic modulus and lower density, the sensitivity of the sensor could significantly be increased. One of such stiff and light-weight materials is boron carbide ( $E = 483$  GPa,  $\rho = 2.52$  g/cm<sup>3</sup> [8, 9]).

Generally all ceramic cantilevers are more sensitive than steel based cantilevers (Fig. 1). For example, boron carbide-based cantilever has the sensitivity about 7 times higher than steel based one. All ceramic cantilevers have also other advantages compared with traditional steel-based cantilevers. They have a higher resistance to cyclic loading and a higher stability in aggressive media.

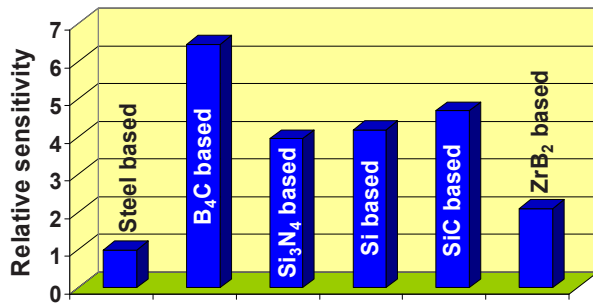


Figure 1. Relative sensitivity of the cantilevers with the same dimensions.

The sensitivity of the microcantilever sensor will increase when its dimensions decrease. As the dimensions of a cantilever are reduced by a factor of  $\alpha$ , the sensitivity is enhanced by a factor of  $\alpha^{-4}$  [5]. However, when such a decrease of dimensions happens, another factor comes into play which needs to be considered. When the piezoelectric layer becomes thinner, at a given applied voltage, the strain mismatch between piezo- and non-piezoelectric layer becomes larger and larger, which could lead to a rise in the residual stresses. When the residual stresses reach a certain critical value, a deterioration of the service properties, due to appearance of the irreversible strain in the piezoelectric layer, or even a complete failure of the sensor will occur. Therefore, the lower dimensional limits for the safe cantilever operation are important to be determined. Static analysis for multi-layered piezoelectric cantilevers were developed in [10]. However, the lower limit of the cantilever size has not been considered.

The goal of this work is to evaluate the lower dimensional limit of a two layer microcantilever sensor, where a piezoelectric layer is made of lead

zirconate titanate ceramic, and a non-piezoelectric layer is made of boron carbide, which is capable to exhibit high sensitivity and good service properties. The evaluation is made by a simplified analytical model based on von Mises criterion and Mohr's strength theory.

## 2. Model Development

### 2.1. MODEL ASSUMPTIONS

A schematic presentation of a microcantilever sensor with defined dimensions of the piezoelectric and non-piezoelectric layers is shown in Fig. 2a. The maximum deflection state of the microcantilever is schematically shown in Fig. 2b, which will be used for the analysis with no intermediate deflections between zero and maximum deformation being considered. Figure 2c presents an orientation of the cantilever with a defined horizon line. These parameters presented in Fig. 2a–c are used for the estimation of the lower limit of the sensor dimensions which are still feasible for the reliable sensor operation. The main assumptions of the model are summarized as follows:

1. Only stress distribution in the clamped cross-section of a cantilever is considered, as it is the most critical one.
2. A cantilever is allowed to expand and compress without any constraints along a  $y$ -direction perpendicular to the layers (Fig. 2a) which results in the stress component in this direction to be equal to zero.
3. The clamped cross-section of the cantilever is assumed to be a plane and it has a rectangular shape for all deformations (Fig. 2a). Therefore, the stress components along a  $z$ -direction perpendicular to the longitudinal axis of the cantilever and parallel to the layers do not change.

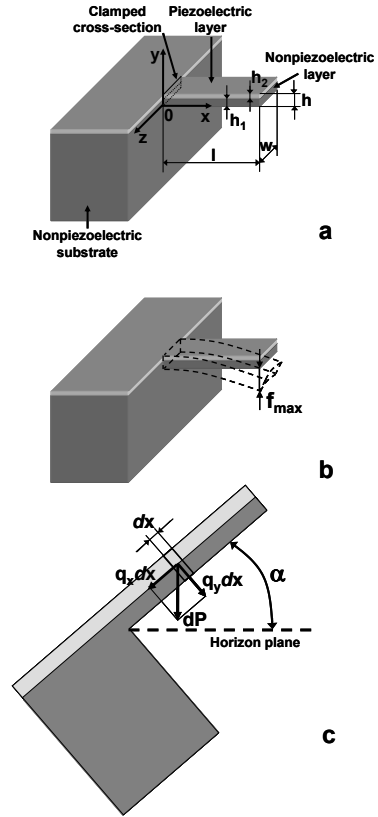


Figure 2. Schematic presentations of cantilever: (a) geometric parameters; (b) state of maximum deflection; (c) orientation of cantilever.

4. Only a cantilever with a maximum deflection  $f_{\max}$  will be evaluated. We name it “a static problem” (Fig. 2b).
5. Only the upper estimate of deflection  $f_{\max}$  of the cantilever free end is considered.
6. The cantilever is analyzed only for the case where the  $z$ -axis is parallel to the horizon plane (Fig. 2c).
7. The mismatch of the coefficients of thermal expansion between the two layers of the cantilever at room temperature is not considered.
8. Shear stresses in a clamped cross-section of the cantilever are neglected since they are substantially smaller than normal stresses analyzed.
9. The interface between two layers is suggested to be indestructible and two layers are bonded rigidly (without sliding).

A simple model which would take into account different parameters of the successful sensor operation is developed which allows the estimation of the minimal dimensions without reaching the critical stress level in the sensor's layers. The model applicability is determined by the deflection criterion:

$$f_{\max} / h < a, \quad (1)$$

where

$f_{\max}$  is the maximum deflection of the cantilever free end (Fig. 2b),

$h$  is the total thickness of cantilever (Fig. 2a), and

$a$  is a prescribed value less than one (0.1 in this work).

The ultimate state of the cantilever can be achieved when at least one of two criteria are fulfilled. The first criterion is applicable to a failure of the non-piezoelectric layer and a second criterion is applicable to the appearance of irreversible strain in the piezoelectric layer. The challenge is to determine the conditions to avoid the ultimate state of the cantilever.

The failure of the non-piezoelectric layer will not occur, according to Mohr's strength theory [11], when the following condition is met:

$$\sigma_M < \sigma_+, \quad (2)$$

where the effective stress  $\sigma_M$  is

$$\sigma_M = \max(\sigma_{x1}, \sigma_{y1}, \sigma_{z1}) - \frac{\sigma_+}{\sigma_-} \min(\sigma_{x1}, \sigma_{y1}, \sigma_{z1}), \quad (3)$$

and

$\sigma_+$  is the tensile strength of the non-piezoelectric material.  $\sigma_+$  can be also evaluated as its bending strength.

$\sigma_-$  is the strength of non-piezoelectric material under compression,

$\sigma_{x1}, \sigma_{y1}, \sigma_{z1}$  are normal stress components in directions  $x, y, z$ , respectively, acting in the non-piezoelectric layer.

The cantilever will also reach its ultimate state when the irreversible strain in the piezoelectric layer appears. The irreversible strain is a result of the ferroelastic domain switching under loading of the piezoelectric material at certain stress levels [12]. The safe stress level which will not result in the appearance of the irreversible deformation can be evaluated using von Mises criterion [13]:

$$\sigma_i < \sigma_0, \quad (4)$$

where

$$\sigma_i = \frac{1}{\sqrt{2}} \sqrt{(\sigma_{x2} - \sigma_{y2})^2 + (\sigma_{y2} - \sigma_{z2})^2 + (\sigma_{z2} - \sigma_{x2})^2} \quad (5)$$

is the stress intensity, where shear stresses are neglected in our consideration,

$\sigma_0$  is the stress at the appearance of the irreversible strain in the piezoelectric material,

$\sigma_{x2}, \sigma_{y2}, \sigma_{z2}$  are normal stress components in directions  $x, y, z$ , respectively, acting in the piezoelectric layer.

## 2.2. MODEL EQUATIONS

To determine the model applicability using deflection criterion Eq. (1) the maximum deflection  $f_{\max}$  of the free end of cantilever should be estimated. The upper estimate of bending deflection of the free end can be made from the assumption that maximum curvature of the cantilever (at clamped end) remains constant along the whole length of the cantilever:

$$f_{\max} = \frac{2}{k_x} \sin^2 \left( \frac{lk_x}{2} \right). \quad (6)$$

where

$k_x$  is the cantilever curvature at a clamped end in the  $x$ - $y$  plane. Expression (6) overestimates the deflection but results in the most reliable evaluation of the model's applicability.

To find the conditions to avoid the ultimate state of the cantilever, the stress distribution in the clamped cross-section of the cantilever should be determined. The stress component  $\sigma_{xi}$  directed along  $x$  axis (perpendicular to the cross-section plane) in the  $i$ -th layer, obtained from a hypothesis of plane sections [14] is as follows

$$\sigma_{xi}(y) = E'_i(\varepsilon_x(0) + k_x y - \Delta\varepsilon_{xi} - \nu_i \Delta\varepsilon_{zi}), \quad (7)$$

where  $E'_i = \frac{E_i}{1 - \nu_i^2}$  ( $i = 1, 2$ ),

$E_1$ ,  $\nu_1$  and  $E_2$ ,  $\nu_2$  are elastic modulus and Poisson's ratio of non-piezoelectric and piezoelectric layers respectively,

$\varepsilon_x(0)$  is the total strain component oriented along the  $x$  axis in the clamped cross-section at  $y = 0$ ,

$\Delta\varepsilon_{xi}$  and  $\Delta\varepsilon_{zi}$  ( $i = 1, 2$ ) are the components of strain which are not connected with stress.  $\Delta\varepsilon_{x1} = \Delta\varepsilon_{z1} = 0$  in the non-piezoelectric layer (thermal strains are neglected in our consideration).  $\Delta\varepsilon_{x2}$  and  $\Delta\varepsilon_{z2}$  are piezoelectric strains in piezoelectric layer. Most PZT films exhibit piezoelectric coefficients  $d_{31} = -58$  pm/V and  $d_{33} = 190$ – $250$  pm/V [15]. Components of piezoelectric strain oriented along  $x$  and  $y$  axes are

$$\Delta\varepsilon_{x2} = \Delta\varepsilon_{z2} = \frac{d_{31}U}{h_2}, \quad (8)$$

$$\Delta\varepsilon_{y2} = \frac{d_{33}U}{h_2}, \quad (9)$$

respectively, where

$U$  is the electric voltage applied to the piezoelectric layer, and

$h_2$  is the thickness of the piezoelectric layer.

The cantilever is allowed to expand and compress without any constraints along the  $y$  axis which results in  $\sigma_{yi} = 0$ . A stress component directed along the  $z$  axis in a clamped cross-section in the  $i$ -th layer can be determined from the condition  $\varepsilon_z = 0$ , where  $\varepsilon_z$  is the total strain oriented along the  $z$  axis and a hypothesis of plane sections as follows:

$$\sigma_{zi}(y) = E'_i[\nu_i(\varepsilon_x(0) + k_x y - \Delta\varepsilon_{xi}) - \Delta\varepsilon_{zi}]. \quad (10)$$

The curvature  $k_x$  and the strain  $\varepsilon_x(0)$  can be found from equilibrium conditions for the cantilever, since only the static problem is analyzed. We have two equilibrium conditions. The first condition is a force balance and the second condition is a moment balance, and both are equal to zero in the clamped cross-section. These two conditions are determined by the system of two linear equations:

$$\begin{cases} w \sum_{i=1}^2 \int_{y_{i-1}}^{y_i} \sigma_{xi}(y) dy + F_x(0) = 0, \\ w \sum_{i=1}^2 \int_{y_{i-1}}^{y_i} \sigma_{xi}(y)(y - y_c) dy + M(0) = 0, \end{cases} \quad (11)$$

where

$\sigma_{xi}(y)$  is determined by Eq. (7),

$w$  is the cantilever width (Fig. 2a),

$y_0 = 0$ ,

$y_1 = h_1$ ,

$y_2 = h_1 + h_2 = h$ ,

$h_1, h_2$  are the thicknesses of non-piezoelectric and piezoelectric layers, respectively (Fig. 2a).

$y_c = \frac{E'_1 h_1^2 + E'_2 (h^2 - h_1^2)}{2(E'_1 h_1 + E'_2 h_2)}$  is the coordinate of the neutral axis in the

clamped cross-section of the cantilever derived from a balance of static moments of the cross-section,

$F_x(0) = -q_x l$  is the longitudinal force in the cantilever clamped end,

$M(0) = \frac{q_y l^2}{2}$  is the bending moment in the clamped cross-section,

$l$  is the cantilever length (Fig. 2a).

$q_x = gw\rho_{eff}h \sin \alpha$  (which can be obtained from the expression for a gravitational force  $dP = gdm = gw\rho_{eff}hdx$  acting on an elementary volume  $whdx$  taking into account the angle  $\alpha$ ) (Fig. 2c),

$q_y = gw\rho_{eff}h \cos \alpha$ ,

$\rho_{eff} = \frac{\rho_1 h_1 + \rho_2 h_2}{h}$  is the effective density of the cantilever,

$\rho_1$  and  $\rho_2$  are densities of the non-piezoelectric and piezoelectric layers, respectively,

$g$  is the gravitational acceleration,

$\alpha$  is the angle between  $x$  axis and the horizon plane (Fig. 2c).

The solution of system of the two linear equations (11) is

$$\varepsilon_x(0) = \frac{B_1 A_{22} - B_2 A_{12}}{A_{11} A_{22} - A_{12}^2}, \quad (12)$$

$$k_x = \frac{B_2 A_{11} - B_1 A_{12}}{A_{11} A_{22} - A_{12}^2}, \quad (13)$$

where

$$A_{11} = E'_1 h_1 + E'_2 (h - h_1),$$

$$A_{12} = \frac{1}{2} [E'_1 h_1^2 + E'_2 (h^2 - h_1^2)],$$

$$A_{22} = \frac{1}{3} [E'_1 h_1^3 + E'_2 (h^3 - h_1^3)],$$

$$B_1 = E'_1 h_1 \Delta \varepsilon_1 + E'_2 (h - h_1) \Delta \varepsilon_2 + \frac{q_x l}{w},$$

$$B_2 = \frac{1}{2} \left[ E'_1 h_1^2 \Delta \varepsilon_1 + E'_2 (h^2 - h_1^2) \Delta \varepsilon_2 + \frac{l}{w} (2y_c q_x - l q_y) \right].$$

Knowing the curvature  $k_x$  and the strain  $\varepsilon_x(0)$  we can evaluate the applicability of the model and determine a stress distribution in the clamped cross-section of the cantilever in order to find the safe conditions of the cantilever operation.

### 3. Results and Discussion

The effective stress and stress intensity in the clamped end of the cantilever have been calculated using Eqs. (7)–(10), (12), and (13). The maximum bending deflection of the cantilever free end has been estimated using Eq. (6). The following geometric considerations have been taken into account for the calculations:  $l/w = 2.6$ ,  $h_1/h = 0.5$ , and  $\alpha = 0$  (Fig. 2). The constant ratio  $l/h = 16.25$  was used for the calculation of critical parameters as a function of the cantilever's length. The cantilever length was taken as  $65 \mu\text{m}$  when



the effect of  $l/h$  and  $h_1/h$  on critical parameters was estimated. While the effective stress and stress intensity in the cantilever's clamped end and the maximum bending deflection of the cantilever free end do not depend on the  $l/w$  ratio, this ratio is used to determine the sensitivity of the cantilever  $\Delta f_n / \Delta m$  (the resonance frequency shift per unit loaded mass) [5]:

$$\frac{\Delta f_n}{\Delta m} = \frac{\nu_n^2}{4\pi} \frac{1}{l^4} \frac{l}{w} \left( \frac{1}{0.236\sqrt{12}\rho_{eff}} \sqrt{\frac{\tilde{E}}{\rho_{eff}}} \right), \quad (14)$$

where

$\nu_n^2$  is the dimensionless  $n$ th-mode eigenvalue,

$$\tilde{E} = \frac{E_1^2 r_1^4 + E_2^2 r_2^4 + 2E_1 E_2 r_1 r_2 (2r_1^2 + 2r_2^2 + 3r_1 r_2)}{E_1 r_1 + E_2 r_2}$$

is the effective elastic modulus, and  $r_1 = h_1/h$  and  $r_2 = h_2/h$ .

The properties of the materials used for the calculation of the effective stress, stress intensity, and maximum bending deflection are presented in Table 1.

TABLE 1. Parameters of layers used in the calculation.

	Elastic modulus $E_i$ , GPa	Poisson ratio $\nu_i$	Density $\rho_i$ , g/cm <sup>3</sup>	Strength $\sigma_+$ , MPa	Yield point $\sigma_0$ , MPa
B <sub>4</sub> C layer	483	0.16	2.52	300	-
PZT layer	61	0.25	7.5	300	10

The dependence of the dimensionless parameters  $\sigma_M/\sigma_+$ ,  $\sigma_i/\sigma_0$  and  $f_{max}/ah$  as a function of the cantilever's length in the clamped cross-section of the cantilever, with an applied voltage of 5 V on the piezoelectric layer are shown in Fig. 3. The ultimate state of the cantilever is shown by the dashed line. The ultimate state will be achieved when one of two characteristic parameters  $\sigma_M$  and  $\sigma_i$  approaches its own limit, i.e.  $\sigma_M = \sigma_+$  and  $\sigma_i = \sigma_0$ . The  $f_{max}/ah$  parameter determines the applicability of the model used in the current work. The  $f_{max}/ah$  is approaching its limit at much smaller cantilever lengths than that of  $\sigma_i$  (Fig. 3), which means that the model is indeed applicable in the area where  $\sigma_i$  reaches its critical value  $\sigma_0$ , and the cantilever reaches its ultimate state.

As one can see from Fig. 3, there is a similar trend for all three parameters ( $\sigma_M/\sigma_+$ ,  $\sigma_i/\sigma_0$ , and  $f_{max}/ah$ ). For example, all three parameters plotted as a function of the cantilever length exhibit a minimum. Such dependencies are determined by two major factors affecting the stresses in the clamped end of the cantilever. The first factor is a piezoelectric strain. If  $l/h$  and  $h_1/h$  ratios are constant, the contribution of the piezoelectric strain becomes more and more significant when the length of the cantilever decreases because of the decrease of the piezoelectric layer thickness. The second factor affecting the stresses in the clamped end of the cantilever is its own weight, which is proportional to its length.

Thus, the smallest geometric dimensions of the cantilever which are safe for reliable operation are those with the level of the stresses in the clamped end of the cantilever lower than the corresponding ultimate stress. It is important to notice that the first

criterion, which is fulfilled as the length of the cantilever decreases, is  $\sigma_i = \sigma_0$  in the piezoelectric layer. It is also clear that the most dangerous points in the clamped cross-section are those which are located at the interface between layers. Thus, the intersection point between  $\sigma_i/\sigma_0|_{y=0.5h} = f(l)$  curve and the dashed line is to the right of the intersection of the dashed line with  $\sigma_i/\sigma_0|_{y=h} = f(l)$ . The failure of the non-piezoelectric layer (criterion  $\sigma_M = \sigma_+$ ) can be achieved at a much smaller length of the cantilever. Therefore, the most detrimental parameter of the safe operation of the cantilever is  $\sigma_i/\sigma_0$  in the clamped cross-section of the piezoelectric layer at the interface between layers.

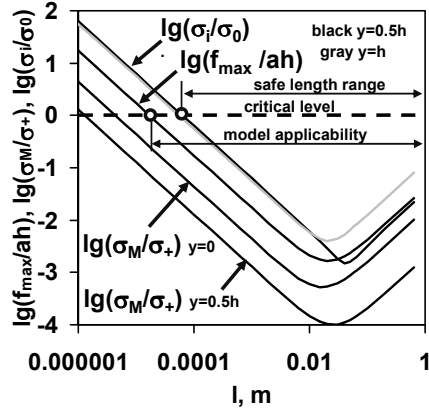


Figure 3. Dependence of cantilever parameters on its length at 5 V.

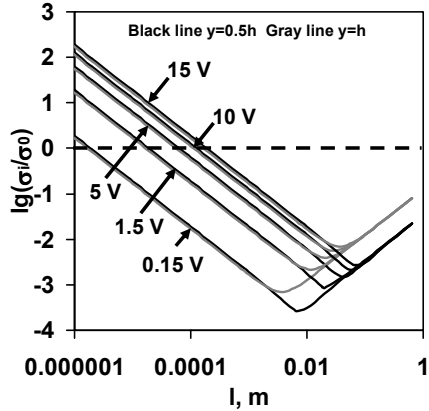


Figure 4. Dependence of stress intensity parameter on cantilever length.

The effect of the applied voltage to the piezoelectric layer on the stress intensity in the clamped cross-section of the piezoelectric layer in two points, where  $y = h$  and  $y = 0.5h$  is shown in Fig. 4. The critical stress intensity with decreasing length is always achieved first at the interface between layers, e.g. when  $y = 0.5h$  for all voltages used in the calculations. The increase of the applied voltage  $U$  significantly influences the stress intensity causing an increase in the critical length of the cantilever, where the condition of the safe stress intensity is still maintained. Thus, the increase of the applied voltage by an order of two, from 0.15 to 15 V, leads to the increase of the critical length of the cantilever by two orders of magnitude, from  $\sim 1.9$  to  $190 \mu\text{m}$ .

Dependences of dimensionless parameters  $\sigma_M/\sigma_+$ ,  $\sigma_i/\sigma_0$  and  $f_{\max}/ah$  on the  $l/h$  ratio in the cantilever's clamped cross-section with an applied voltage of 5 V on the piezoelectric layer are shown in Fig. 5, which are presented as straight lines in the bilogarithmic scale. All three parameters approach and exceed the critical level equal to zero as the  $l/h$  ratio increases, e.g. if the cantilever's thickness decreases but the length remains constant. The most important parameter is again  $\sigma_i/\sigma_0$  since it reaches the critical value before any other parameter, when  $l/h$  ratio is the smallest.

The effect of the applied voltage to the piezoelectric layer and the  $l/h$  ratio on the dimensionless stress intensity in the clamped cross-section of the piezoelectric layer is presented in Fig. 6. The higher voltage results in larger values of  $\sigma_i/\sigma_0$  parameter, meaning that the appearance of the irreversible strain is facilitated by the increase in applied voltage. At the given voltage the stress intensity is always higher at the interface between piezoelectric and non-piezoelectric layers than that at the free surface of the piezoelectric layer. Therefore, for a given voltage and cantilever's length the ultimate cantilever's thickness exists below which the cantilever's operation becomes unsafe and non-reliable. For example, the ultimate thickness is equal to  $3.87 \mu\text{m}$  at the applied voltage of 5 V and  $65 \mu\text{m}$  of the cantilever's length.

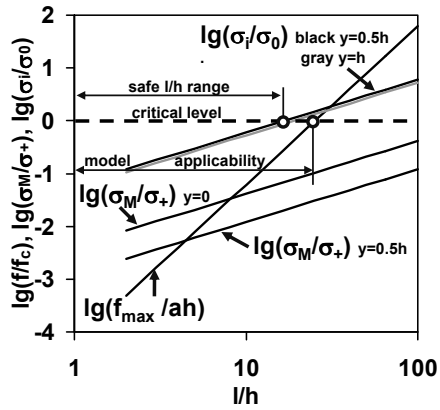


Figure 5. Dependence of cantilever parameters on the ratio  $l/h$  at 5 V.

Dependences of dimensionless parameters on relative thickness of the non-piezoelectric layer (its thickness divided by total thickness of the cantilever) in the cantilever's clamped cross-section for voltage of 5 V are shown in Fig. 7. Only stress intensity riches values higher than critical level. Lower voltage results in higher critical relative thickness of the non-piezoelectric layer and, in such a way, lower relative thickness of the piezoelectric layer (Fig. 8).

One can show that increasing the stress level  $\sigma_0$ , when the irreversible deformation will show up in a piezoelectric material (for example, by pre-polarization [15]), decreases the ultimate cantilever size. For example, increasing  $\sigma_0$  by a factor of 3 results in an ultimate length of 0.65  $\mu\text{m}$ . This corresponds to a cantilever sensitivity of about  $5 \cdot 10^{24}$  Hz/kg according to Eq. (14). If a detectable frequency shift is 10 Hz, the minimum detectable mass in this case is about  $18 \cdot 10^{-24}$  kg, which is approximately the mass of 6 atoms of mercury. The calculations of cantilever sensitivity using (14) have also shown that, if the sensitivity of the steel-based microcantilever is taken as 1, the replacement of steel with  $\text{B}_4\text{C}$  ceramics will increase the sensitivity by a factor of about seven.

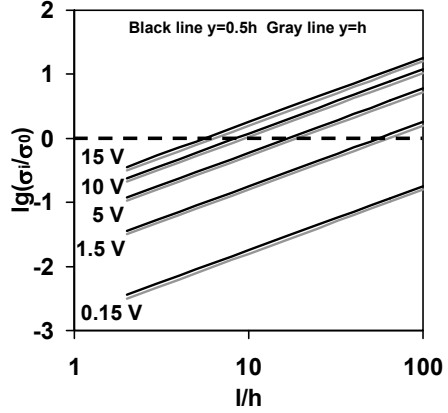


Figure 6. Dependence of stress intensity parameter on the ratio  $l/h$ .

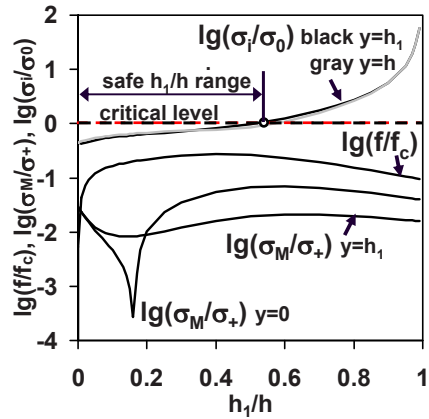


Figure 7. Dependence of cantilever parameters on the ratio  $h_1/h$  at 5 V.

#### 4. Conclusions

As a result of our study, a model has been developed which allows an estimation of the dimensional limits of the two layer microcantilever sensors. The model applicability for all considered cantilever lengths has been verified using the maximum deflection criterion proposed in this work.

It was shown for cantilever parameters used for the calculation that von Mises criterion places more serious restrictions on the cantilever length compared to the Mohr's theory of strength, therefore it should be satisfied first. In the proposed model, a stress distribution in the clamped cross-section of cantilever does not depend on the cantilever's width.

It was shown that the stress intensity in the clamped cross-section has different trends as a function of the cantilever length. Thus, for small length range, the stress intensity is increasing as length is decreasing, but for the larger lengths, the stress intensity is increasing as the length is increasing. The stress intensity has a minimum at some intermediate value of the length. The dependence of stress intensity on the cantilever length can be conditionally split into three different ranges, which can be found in the plots obtained for all applied voltage values. The first range is for the small cantilever lengths, where the effect of the self weight is negligibly small. In the opposite range, where the lengths are large, the piezoelectric strain will have minor effects on the stress intensity in comparison with the self weight of the cantilever. In the length's interval between these two ranges, where there is a minimum of the stress intensity, the piezoelectric strain and the effect of the self weight are comparable.

The critical minimal cantilever length could be found when other conditions, such as applied voltage, material parameters, and the thickness ratio of the two layers, are held constant. When the length of the cantilever decreases, the irreversible strain in the piezoelectric layer at a given voltage increases. Thus, at a certain critical cantilever length, the appearance of irreversible strain will result in unsafe cantilever operation. For a given applied voltage and cantilever's length the ultimate cantilever's thickness exists below which the cantilever's operation becomes unsafe and non-reliable as well. The higher voltage results in increased values of the ultimate thickness. At a given voltage, the stress intensity is always higher at

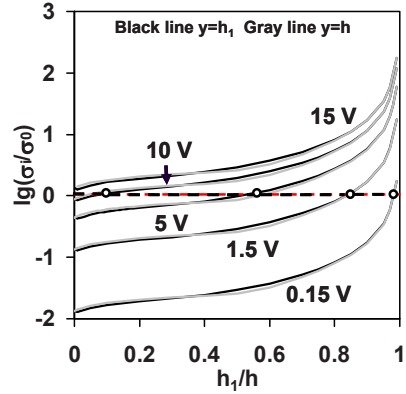


Figure 8. Dependence of stress intensity parameter on the ratio  $h_1/h$ .

the interface between layers than at the free surface of the piezoelectric layer.

## Acknowledgement

This work was supported by NATO Collaborative Linkage Grant “Layered ceramic sensors for biological and chemical detection” and NATO ARW Grant “Boron Rich solids: Sensors for Biological and Chemical Detection, Ultra-high Temperature Composites, Thermoelectrics, Armor”.

## References

1. H.-J. Butt, P. Siedle, K. Seifert, T. Seeger, K. Fendler, E. Bamberg, K. Goldie, and A. Engel, Scan Speed Limit in Atomic Force Microscopy, *Journal of Microscopy*, vol. 169, pp. 75–84, 1993.
2. P.I. Oden, Gravimetric Sensing of Metallic Deposits Using an End-Loaded Microfabricated Beam Structure, *Sensors and Actuators B*, vol. 53, pp. 191–196, 1998.
3. W.Y. Shih, X. Li, H. Gu, W.H. Shih, and I.A. Aksay, Simultaneous Liquid Viscosity and Density Determination with Piezoelectric Unimorph Cantilevers, *Journal of Applied Physics*, vol. 89, pp. 1497–1505, 2001.
4. J.W. Yi, W.Y. Shih, R. Mutharasan, and W.-H. Shih, In Situ Cell Detection Using Piezoelectric Lead Zirconate Titanate – Stainless Steel Cantilevers, *Journal of Applied Physics*, vol. 93, pp. 619–625, 2003.
5. J.W. Yi, W.Y. Shih, and W.-H. Shih, Effect of Length, Width, and Mode on the Mass Detection Sensitivity of Piezoelectric Unimorph Cantilevers, *Journal of Applied Physics*, vol. 91, pp. 1680–1686, 2002.
6. B. Ilic, D. Czaplewski, H.G. Craighead, P. Neuzil, C. Campagnolo, and C. Batt, Mechanical Resonant Immunospecific Biological Detector, *Applied Physics Letters*, vol. 77, pp. 450–452, 2000.
7. T. Thundat, E.A. Wachter, S.L. Sharp, and R.J. Warmack, Detection of Mercury Vapor Using Resonating Microcantilevers, *Applied Physics Letters*, vol. 66, pp. 1695–1697, 1995.
8. N. Orlovskaya, M. Lugovy, V. Subbotin, O. Radchenko, J. Adams, M. Chheda, J. Shih, J. Sankar, and S. Yarmolenko, Robust Design and Manufacturing of Ceramic Laminates with Controlled Thermal Residual Stresses for Enhanced Toughness, *Journal of Materials Science*, vol. 40, pp. 5483–5490, 2005.
9. G. de With, High Temperature Fracture of Boron Carbide: Experiments and Simple Theoretical Models, *Journal of Materials Science*, vol. 19, pp. 457–466, 1984.
10. H.J. Xiang, and Z.F. Shi, Static Analysis for Multi-Layered Piezoelectric Cantilevers, *International Journal of Solids and Structures*, vol. 45, pp. 113–128, 2008.
11. S. Timoshenko, *Strength of Materials*, 3rd ed, Krieger Publishing Company, 1976.
12. S.C. Hwang, and R.M. McMeeking, A Finite Element Model of Ferroelastic Polycrystals, *International Journal of Solids and Structures*, vol. 36, pp. 1541–1556, 1999.

13. A. Nadai, Theory of Flow and Fracture of Solids, Vol. 1, McGraw-Hill, New York, 1950.
14. S.P. Timoshenko, and J.N. Goodier, Theory of Elasticity, McGraw-Hill, New York, 1970.
15. Z. Shen, W.Y. Shih, and W.-H. Shih, Self-Exciting, Self-Sensing  $\text{PbZr}_{0.53}\text{Ti}_{0.47}\text{O}_3/\text{SiO}_2$  Piezoelectric Microcantilevers with Femtogram/Hertz Sensitivity, Applied Physics Letters, vol. 89, 023506, 2006.

Boron Rich Solids

Sensors, Ultra High Temperature Ceramics,  
Thermoelectrics, Armor

Orlovskaya, N.; Lugovy, M. (Eds.)

2011, XVIII, 330 p., Hardcover

ISBN: 978-90-481-9817-7